

## Metal-to-Semiconductor Transition in Squashed Armchair Carbon Nanotubes

Jun-Qiang Lu,<sup>1,2</sup> Jian Wu,<sup>1</sup> Wenhui Duan,<sup>2</sup> Feng Liu,<sup>3</sup> Bang-Fen Zhu,<sup>1</sup> and Bing-Lin Gu<sup>1,2</sup>

<sup>1</sup>Center for Advanced Study, Tsinghua University, Beijing 100084, People's Republic of China

<sup>2</sup>Department of Physics, Tsinghua University, Beijing 100084, People's Republic of China

<sup>3</sup>Department of Materials Science and Engineering, University of Utah, Salt Lake City, Utah 84112

(Received 13 January 2003; published 18 April 2003)

We investigate electronic transport properties of the squashed armchair carbon nanotubes, using tight-binding molecular dynamics and the Green's function method. We demonstrate a metal-to-semiconductor transition while squashing the nanotubes and a general mechanism for such a transition. It is the distinction of the two sublattices in the nanotube that opens an energy gap near the Fermi energy. We show that the transition has to be achieved by a combined effect of breaking of mirror symmetry and bond formation between the flattened faces in the squashed nanotubes.

DOI: 10.1103/PhysRevLett.90.156601

PACS numbers: 72.80.Rj, 73.22.-f, 73.23.-b, 85.35.Kt

The discovery of carbon nanotubes [1] has stimulated intensive research interest, partly because of their unique electronic properties and their potential application in nanodevices. In particular, much effort has been made to manipulate the low-energy electronic properties of carbon nanotubes, as it is the requisite step for using nanotubes to realize a functional device.

A single-walled nanotube (SWNT) can be either semiconducting or metallic depending on its diameter and helicity [2]. A tube is metallic if the Fermi  $k$  point of the corresponding graphene sheet, from which the tube is wrapped, remains as an allowed  $k$  point by the periodic boundary condition for the tube; otherwise, it is semiconducting. Consequently, most previous studies have focused on a popular idea of modifying the electronic properties of SWNTs by structural perturbation, in an attempt to shift the Fermi  $k$  point away from an allowed state, resulting in a metal-to-semiconductor transition (MST).

Various experimental methods, such as twisting [3], introducing topological defects [4], and stretching [5], have been used to manipulate the electronic and transport properties of nanotubes. Theoretical studies [6–8] have also been performed to help explore the correlation between the structural perturbation and the change of electronic properties. However, in general, the experiments are done in a guesswork manner, because it is *a priori* unknown how a given structural perturbation would change the electronic properties. One major difficulty is that the structural perturbation occurs for atoms in real space, but the change of electronic properties has to be revealed by electronic bands in reciprocal space.

In this Letter, we demonstrate a new method of manipulating electronic properties of SWNTs by examining directly the atomic structural perturbation in real space without the need of analyzing the bands in reciprocal space. We show that, when a structural perturbation makes the two original equivalent sublattices in a metallic armchair SWNT distinguishable, it will open an energy gap, leading to a MST. This can be achieved, for

example, by simply squashing the tube. Furthermore, we show that the *physical* distinction of the two sublattices must be achieved by a combined effect of mirror-symmetry breaking (MSB) and bond formation between the flattened faces of the squashed tubes, while neither the MSB nor the bonding alone would result in the MST.

We demonstrate the basic principles of our method by squashing an armchair (8, 8) SWNT, as shown in Fig. 1. The simulations, for both structural optimization and calculation of electronic transport property, are performed using a four-orbital tight-binding (TB) method. To squash the tube, two identical tips with a width of  $d_x = 5.80 \text{ \AA}$  are used to press the tube symmetrically about its

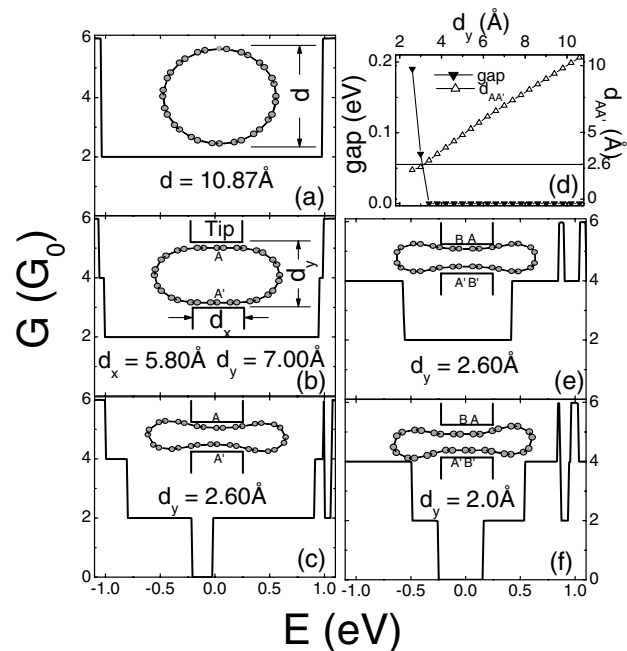


FIG. 1. (a)–(c),(e),(f) Conductances of various nanotube structures, which are shown as the insets.  $E$  is the energy of injected electrons, and the Fermi energy of the ideal armchair (8, 8) nanotube is taken as zero. (d) The conductance gap and  $d_{AA'}$  as a function of the tip distance  $d_y$ .

center in the  $\pm y$  direction, as shown in Fig. 1(b). The tips are assumed to be super stiff with a hard-wall interaction with the tube. At each tip position, the atomic structure, i.e., the shape of the tube, is optimized [9]. Most noticeably, as the tube is pressed, its cross section changes from a circle to an ellipse [Fig. 1(b)] and then to a dumbbell [Fig. 1(c)]. As long as the distance between the two tips is not too short ( $> 1.8 \text{ \AA}$ ), the tube is found to maintain its structural integrity, and the whole process is reversible. Further pressing of the tips to shorter distances ( $< 1.8 \text{ \AA}$ ) would permanently damage the tube.

Using the optimized structure at all tip positions, we employ the TB Green's function method [10–12] to study the electronic transport properties of the squashed tubes. Within the framework of the Landauer approach, the conductance is expressed as  $G = G_0 \text{Tr}(\Gamma_L \mathcal{G}_C \Gamma_R \mathcal{G}_C^\dagger)$  [13,14], where  $G_0 (= 2e^2/h)$  is the unit quanta of conductance,  $\mathcal{G}_C$  is the Green's function of the conductor, and  $\Gamma_L$  and  $\Gamma_R$  are the spectral density describing the coupling between the leads and the conductor.

The typical conductance curve of a perfect armchair (8, 8) SWNT is shown in Fig. 1(a). It represents a metallic behavior, which is well known for armchair SWNTs. The conductance near the Fermi energy  $E_F$  is  $2G_0$ , indicating that there are two conducting channels. For the squashed tube, we consider two different cases: one breaking the mirror symmetry (MS) about the  $y$  axis [Figs. 1(b) and 1(c)] and the other preserving the MS [Fig. 1(e)].

When the tube is squashed without MS, its conductance remains at  $2G_0$  near  $E_F$  with an elliptical shape [Fig. 1(b)], but drops sharply to zero with a dumbbell shape [Fig. 1(c)]. Thus, a MST can be achieved by squashing the tube, but only after the tube is squashed to a dumbbell shape. The physical difference is that the two flattened faces of an elliptical tube remain separate without bonding (atomic-orbital overlap), while they become close enough in a dumbbell tube to form new bonds (see discussion below). It has been suggested that the MSB may lead to opening an energy gap in a metallic armchair SWNT [6]. However, Fig. 1(b) clearly shows that the MSB by itself cannot open an energy gap and its only effect is to cause a slight variation in the conductance step. A gap may be opened only after the atomic orbitals on the two flattened faces of the squashed tube, without MS, overlap with each other to form new bonds.

To quantify the degree of squashing in terms of the bonding between the two flattened faces, we monitor the distance between the two closest atoms,  $d_{AA'}$ ,  $A$  in the upper face and  $A'$  in the lower face, as shown in Fig. 1(b). In Fig. 1(d), we plot the conductance gap near  $E_F$  and  $d_{AA'}$ , as a function of the tip separation  $d_y$ . Clearly, the conductance gap appears when  $d_{AA'} < 2.6 \text{ \AA}$ . As a cutoff length of  $2.6 \text{ \AA}$  for the C-C bond is used [10], it indicates that the gap is only opened after the atom  $A$  starts to form a bond with the atom  $A'$ . This is further confirmed by plotting of charge density, as shown in Fig. 2. It can be vividly seen that the charge density

overlaps between the two flattened faces in the dumbbell tube [Fig. 2(b)], reflecting the new bonding between atoms  $A$  and  $A'$ . In contrast, no density overlap and, hence, bonding occurs in the elliptical tube [Fig. 2(a)].

The above results of the squashed tubes without MS demonstrate that bond formation between the flattened faces plays an important role in driving the MST. However, it remains unknown whether such bonding alone is sufficient to induce the MST, i.e., whether the MSB also plays a role, as suggested before [6,15]. To test this, we take a look at the squashed tubes preserving the MS, as shown in Fig. 1(e). Interestingly, the conductance remains at  $2G_0$  near  $E_F$ , even when the distance between the two flattened faces is less than  $2.60 \text{ \AA}$ . This indicates that the MST cannot be induced by the bonding, if the MS is preserved. [The bonding between the two flattened faces is also reflected by the charge density distribution in Fig. 2(c).] Thus, we conclude that the MST can be driven by neither the MSB nor the bonding alone; it has to be driven by the combined effect of the two.

Next we show that the combined effect of the MSB and the bonding between the flattened faces in a squashed armchair SWNT is to make the two original equivalent sublattices in the tube distinguishable, and such distinction can then be used as a unique condition for driving the MST. It is well known that the graphene sheet and, hence, the nanotube have two equivalent sublattices, which we may label as  $A$  and  $B$  sublattices. The operation of squashing can then be defined in reference to them. If the  $y$  axis, along which we squash the tube, is chosen to pass through two atoms from the same  $A$  (or  $B$ ) sublattice, as is the case

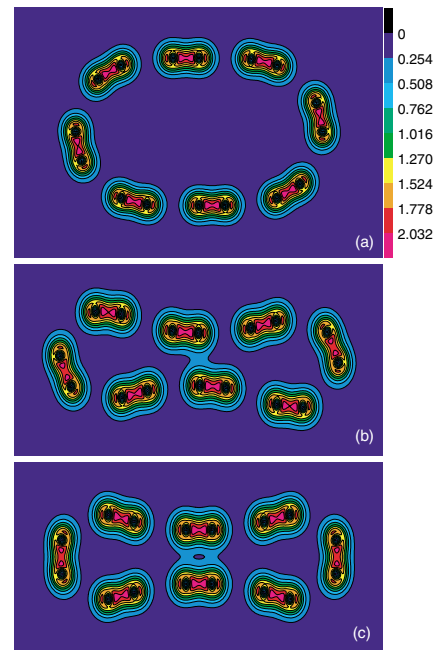


FIG. 2 (color online). Contour plots of the charge density (unit:  $e/\text{\AA}^3$ ) in the cross section of the nanotube structures in Figs. 1(b), 1(c), and 1(e).

in Figs. 1(b) and 1(c), the squashed tube will break the MS about the  $y$  axis. Upon the atomic-orbital overlap between the two flattened faces,  $A$  atoms bond with  $A$  atoms [Fig. 2(b)]. If the  $y$  axis is chosen to pass through two atoms from different sublattices (one from  $A$  and the other from  $B$ ), as is the case in Fig. 1(e), the squashed tube will maintain the MS. Upon the atomic-orbital overlap,  $A(B)$  atoms bond with  $B(A)$  atoms [Fig. 2(c)]. In the following, we refer to the first case as the  $AA'$  structure [Figs. 1(c) and 2(b)] and the second as the  $AB'$  structure [Figs. 1(e) and 2(c)]. Note the two differ by a rotation of  $7.5^\circ$  about the  $y$  axis.

For an ideal armchair (8, 8) SWNT, its metallic behavior can be understood from its energy dispersion relations within a simple  $pp\pi$  model [16]:

$$E_q(k) = \pm \gamma_0 \{1 \pm 4 \cos(q\pi/8) \times \cos(ka/2) + 4 \cos^2(ka/2)\}^{1/2},$$

$$(-\pi < ka < \pi; q = 1, \dots, 8), \quad (1)$$

where  $k$  is the wave vector along the  $z$  axis,  $a = 2.46 \text{ \AA}$  is the lattice constant, and  $\gamma_0$  is the nearest-neighbor hopping integral. The energy dispersion relations near  $E_F$  are shown in Fig. 3(a). The two lines, crossing at the Fermi point, correspond to the two eigenstates (bonding  $\pi$  and antibonding  $\pi^*$ ) with the quantum number  $q = 8$ , as all eight atoms in one sublattice have the same phase. The phase relations between the nearest-neighbor atoms at the Fermi vector  $k_F (= \pm 2\pi/3)$  are shown in Fig. 3(b). The states  $\pi$  and  $\pi^*$  within the tube cross section are shown in Fig. 3(c). Note that the interaction energies between the two sublattices cancel out each other by symmetry, leading to a zero total interaction energy:  $\gamma_0 e^{i(\varphi_B - \varphi_A)} (1 + e^{-i2\pi/3} + e^{-i4\pi/3}) = 0$ . This cancellation, independent of the phase difference ( $\varphi_B - \varphi_A$ ), leads to the degeneracy of the eigenstates  $\pi$  and  $\pi^*$  at  $k_F$ .

We next extend the above model by including the interaction (bonding) between the two flattened faces in a squashed nanotube, using a perturbation Hamiltonian [15]

$$H'(k) = \begin{pmatrix} \delta_{\pi\pi}(k) & \delta_{\pi\pi^*}(k) \\ \delta_{\pi^*\pi}(k) & \delta_{\pi^*\pi^*}(k) \end{pmatrix}. \quad (2)$$

The diagonal matrix elements  $\delta_{\pi\pi}$  and  $\delta_{\pi^*\pi^*}$  merely act to shift the location of the  $\pi$  and  $\pi^*$  bands and, hence, the energy and location of band crossing. It is the off-diagonal elements  $\delta_{\pi\pi^*}$  and  $\delta_{\pi^*\pi}$  that cause quantum mechanical level repulsion and, hence, open an energy gap.

If a MS exists, such as in the  $AB'$  structure, the mirror operator  $M$  must be applied: we have  $M(\pi) = \pi$ ;  $M(H') = H'$ ;  $M(\pi^*) = -\pi^*$ . Then  $\delta_{\pi\pi^*} = M(\delta_{\pi\pi^*}) = M(\langle \pi | H' | \pi^* \rangle) = -\langle \pi | H' | \pi^* \rangle = -\delta_{\pi\pi^*}$ , which gives  $\delta_{\pi\pi^*} = 0$ . Thus, if the MS is preserved, the off-diagonal elements are always zero and the band crossing persists without gap opening, regardless of whether a bond exists between the two flattened faces. This indicates that

the MSB is a necessary (but not sufficient) condition for the MST.

The bonding configuration between the two states  $\pi$  and  $\pi^*$  for the two structures  $AA'$  and  $AB'$  is shown in Fig. 3(d). For the  $AA'$  structure, the off-diagonal element consists of two  $\sigma$  bonds as  $\delta_{\pi\pi^*} = \langle p | H' | p \rangle + \langle p | H' | p \rangle \neq 0$ , where  $|p\rangle$  is the carbon  $2p_y$  orbital. In contrast, for the  $AB'$  structure, it consists of four  $\sigma$  bonds, which cancel out as  $\delta_{\pi\pi^*} = (-\langle p | H' | p \rangle + \langle p | H' | p \rangle) + (\langle p | H' | p \rangle - \langle p | H' | p \rangle) = 0$ . So the off-diagonal element for the  $AB'$  structure is always zero, in agreement with the mirror-symmetry analysis discussed above.

The above analysis clearly demonstrates that the MST must be driven by a combination of the MSB and the bond formation, which effectively distinguishes the two originally equivalent sublattices ( $A$  and  $B$ ). Without the bonding, the two sublattices are always equivalent. Upon the bonding, the two remain equivalent if the MS is preserved, because the bonding occurs between atoms from two sublattices in a symmetric manner, but become distinguishable if the MS is broken, because the bonding

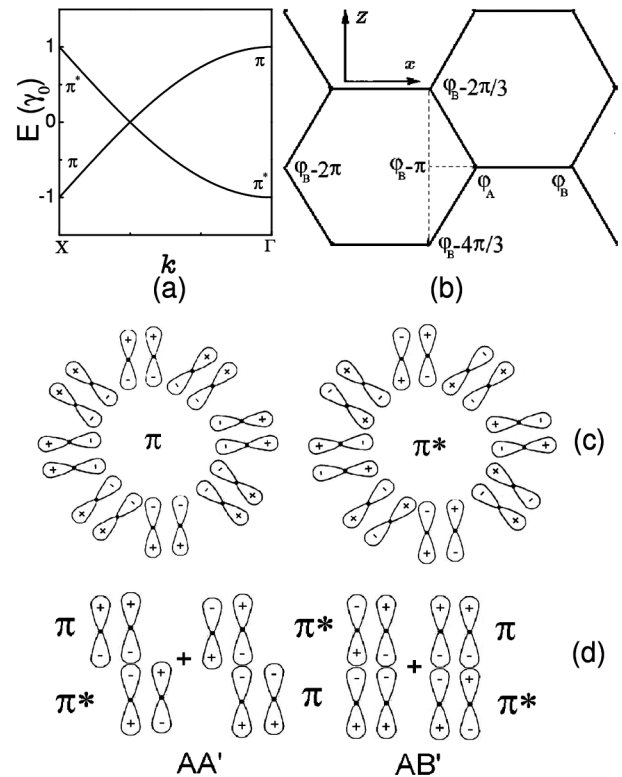


FIG. 3. (a) The energy dispersion relations near  $E_F$  of an ideal armchair (8, 8) SWNT with a  $pp\pi$  model. (b) The phase correlations at  $k_F$  between the three equivalent atomic positions  $B$  that are the nearest neighbors of the atomic positions  $A$ . (c) A schematic representation of the states  $\pi$  and  $\pi^*$  within the cross section of the tube with  $q = 8$ . (d) Configurations of the new bonds formed between the two states  $\pi$  and  $\pi^*$  for structures  $AA'$  and  $AB'$ . The  $AA'$  structure consists of two  $\sigma$  bonds between  $A$  and  $A'$ ; the  $AB'$  structure consists of two  $\sigma$  bonds and two  $\sigma$  antibonds between  $AB'$  and  $A'B$ .

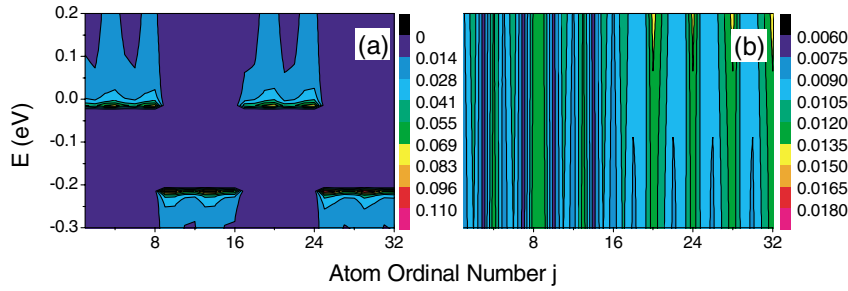


FIG. 4 (color online). The LDOS (unit:  $\text{eV}^{-1}$ ) distributions near  $E_F$  over two atomic layers of the nanotubes for  $AA'$  (a) and  $AB'$  (b) structures. The atoms in the  $B$  ( $A$ ) sublattice are labeled 1 (9) through 8 (16) for the first atomic layer and 17 (25) through 24 (32) for the second atomic layer.

occurs between atoms within only one sublattice ( $A$ ), making it different from the other sublattice ( $B$ ).

Such a distinction of the two sublattices is further revealed by the local density of states (LDOS), as shown in Fig. 4. The LDOS is defined as [11]  $\text{LDOS}(j, E) = -\frac{1}{\pi} \text{Im} \mathcal{G}_C(j, j, E)$ , where  $j$  is the atom index in the nanotube. In Fig. 4, the LDOS of two atomic layers (along the  $z$  axis) are plotted at an energy interval from  $-0.3$  to  $0.2$  eV. Each layer consists of two sublattices ( $A$  and  $B$ ) of 16 atoms. For an ideal tube, the LDOS near  $E_F$  are homogeneously distributed over the two equivalent sublattices  $A$  and  $B$ . For a squashed tube, in an  $AA'$  structure [Fig. 4(a)], the bonding between atoms  $A$  and  $A'$  distinguishes sublattice  $A$  from  $B$ , resulting in a redistribution of the LDOS. Specifically, the electrons tend to distribute around  $A$  sites below  $E_F$ , but around  $B$  sites above it. This causes a discontinuity in the energy spectrum, as shown in Fig. 4(a). In contrast, in  $AB'$  structure [Fig. 4(b)], the LDOS crosses  $E_F$  continuously because the off-diagonal elements are zero and the states  $\pi$  and  $\pi^*$  continue to be the eigenstates. The inhomogeneity of the LDOS in Fig. 4(b) is caused by the inhomogeneous curvature of the squashed nanotube.

Last, we show that squashing the armchair SWNT can be used as a general approach to drive the MST, which is practically important. It would be rather inconvenient if the MST can be driven only by squashing the tube along a specific direction breaking the MS. Fortunately, we find that the MST can, in fact, be driven by squashing the tube along any direction. In case one starts with squashing the tube along a direction that preserves the MS, all that needs to be done is to squash the tube to a larger extent, to a point where spontaneous symmetry breaking occurs. Figure 1(f) shows that for  $AB'$  structure, if one continues to press the tips beyond Fig. 1(e) ( $d_y = 2.60 \text{ \AA}$ ) to Fig. 1(f) ( $d_y = 2.00 \text{ \AA}$ ), a gap near  $E_F$  will eventually appear, because of the spontaneous breaking of MS, causing the two sublattices to be distinguishable.

In summary, we demonstrate that squashing the armchair SWNT can be used as a general approach to induce a MST, which may find practical applications in novel nanodevices, such as for a mechanical nanoswitch. The underlying mechanism is to make the two originally equivalent sublattices in the tube distinguishable, which

requires a combined effect of MSB and bond formation between the two flattened faces in the squashed tube. Such distinction of two sublattices is likely to be generally responsible for the semiconductor behavior of certain classes of nanotubes, such as boron-nitride nanotubes. Besides squashing the tube, other methods, such as chemical adsorption, might be used to distinguish the two sublattices and, hence, to induce the MST.

This work is supported by the Ministry of Education of China, the National High Technology Research and Development Program of China (Grant No. 2002AA311153), and the National Key Program of Basic Research Development of China. F. L. thanks support from U.S.-DOE (Grant No. DE-FG03-01ER45875) and the Natural Science Foundation of China (Grant No. 69928403).

- 
- [1] S. Iijima, *Nature (London)* **354**, 56 (1991).
  - [2] J.W. Mintmire, B. I. Dunlap, and C.T. White, *Phys. Rev. Lett.* **68**, 631 (1992); N. Hamada, S.I. Sawada, and A. Oshiyama, *Phys. Rev. Lett.* **68**, 1579 (1992).
  - [3] C.L. Kane and E.J. Mele, *Phys. Rev. Lett.* **78**, 1932 (1997).
  - [4] L. Chico *et al.*, *Phys. Rev. Lett.* **76**, 971 (1996).
  - [5] V.H. Crespi, M.L. Cohen, and A. Rubio, *Phys. Rev. Lett.* **79**, 2093 (1997).
  - [6] C.J. Park, Y.H. Kim, and K.J. Chang, *Phys. Rev. B* **60**, 10 656 (1999).
  - [7] A. Maiti, A. Svizhenko, and M.P. Anantram, *Phys. Rev. Lett.* **88**, 126805 (2002).
  - [8] P.E. Lammert, P. Zhang, and V.H. Crespi, *Phys. Rev. Lett.* **84**, 2453 (2000).
  - [9] C.H. Xu, C.Z. Wang, C.T. Chan, and K.M. Ho, *J. Phys. Condens. Matter* **4**, 6047 (1992).
  - [10] J.C. Charlier, Ph. Lambin, and T.W. Ebbesen, *Phys. Rev. B* **54**, R8377 (1997).
  - [11] J. Wu *et al.*, *Phys. Rev. Lett.* **80**, 1952 (1998).
  - [12] J. Wu *et al.*, *Appl. Phys. Lett.* **77**, 2554 (2000).
  - [13] H. Chen *et al.*, *Phys. Rev. B* **67**, 113408 (2003).
  - [14] S. Datta, *Transport in Mesoscopic Systems* (Cambridge University Press, Cambridge, 1995).
  - [15] P. Delaney *et al.*, *Nature (London)* **391**, 466 (1998).
  - [16] R. Saito, M. Fujita, G. Dresselhaus, and M.S. Dresselhaus, *Phys. Rev. B* **46**, 1804 (1992).